Factorial Experimental Design on Synthesis of Functional Core/Shell Polymeric Nanoparticles via Differential Microemulsion Polymerization

Chaiwat Norakankorn,[1] Qinmin Pan,[2] Garry L. Rempel,[2] Suda Kiatkamjornwong[3]

[1]*Department of Materials Science, Faculty of Science, Chulalongkorn University, Bangkok, Thailand*
[2]*Department of Chemical Engineering, Faculty of Engineering, University of Waterloo, Ontario, Canada*
[3]*Department of Imaging and Printing Technology, Faculty of Science, Chulalongkorn University, Bangkok, Thailand*

Received 14 February 2009; accepted 27 September 2009
DOI 10.1002/app.31493
Published online 23 December 2009 in Wiley InterScience (www.interscience.wiley.com).

ABSTRACT: Functionalized core/shell nanoparticles of the co-polymer of methyl methacrylate (MMA) and glycidyl methacrylate (GMA) could be polymerized by differential microemulsion polymerization, using a small amount of surfactant (the weight ratio of sodium dodecyl sulfate (SDS)/monomer is 1 : 24). The core/shell nanoparticles have a high conversion, high molecular weight, and small particle size (25–30 nm). The statistical analysis indicated that SDS, water, and the interactionbetween SDS and water have a significant positive interaction between the MMA conversion to form the core nanoparticles. For the core-shell polymer, [GMA], [GMA]*[SDS], and [GMA]*[water] have significant negative effects on conversion; whereas [SDS] and [water], [SDS]*[water] and [GMA]*[SDS]*[water] have positive effects on the conversion to form core/shell nanoparticles. © 2009 Wiley Periodicals, Inc. J Appl Polym Sci 116: 1291–1298, 2010

Key words: core-shell polymer; emulsion polymerization; micelles; nanolayer; particle nucleation

INTRODUCTION

Nanosized functional polymers are interesting nanomaterials for biomedical applications and biotechnology applications, since many biological molecules are compatible with a variety of reactive functional groups. Functional polymer nanoparticles with core/shell structure are one of the interesting substrates resulting from the modification of the surface of the core polymer nanoparticles because high performance functional polymer nanoparticles with core/shell structure can be obtained even though a lower amount of functional monomer is incorporated. Many types of chemical functionalization are indeed available within biomolecules especially amine, thiol, carboxyl, hydroxyl, guanidine, and imidazole groups. Among the various functional polymeric materials, glycidyl-functional polymeric materials are especially interesting because of their excellent properties, such as good adhesion with various substrates and easy modification with many types of functional groups via simple chemical reactions.[1,2] The dispersion copolymerization between methyl methacrylate (MMA) and glycidyl methacrylate (GMA) has been studied.[3] The nonporous microparticles of MMA copolymerized with GMA were prepared by dispersion polymerization.[3] The particle size was found to decrease from 4.2 to 2.1 μm with an increasing mass ratio of GMA/MMA but led to a decrease in glycidyl functional group density on the particle surface.[3] The higher reactivity of the GMA monomer than that of the MMA monomer results in GMA/MMA firstly copolymerized inside the core particle.[3] Thus, a low epoxy group density on the surface of GMA/MMA copolymer particle was obtained. The increments of the glycidyl functional group density on the surface of polymer particle could possibly be achieved by the reduction of the particle from a micrometer scale to a nanometer range since a nanoparticle has a much higher specific surface area than that of a microparticle.

Microemulsion polymerization is a technique that provides colloidal polymer particles with diameters usually smaller than 50 nm dispersed in a continuous aqueous phase.[4] Nevertheless, batch microemulsion polymerization has two major drawbacks which limit its broad application, i.e., (1) low monomer/surfactant weight ratios, usually <1, and (2) low polymer content, usually less than 10 wt %. One approach for overcoming these drawbacks is to carry

Correspondence to: S. Kiatkamjornwong (ksuda@chula.ac.th) and G. L. Rempel (grempel@cape.uwaterloo.ca).

Contract grant sponsor: Thailand Research Fund (TRF); contract grant number: PHD/0269/2545.

Contract grant sponsor: Natural Sciences and Engineering Research Council of Canada (NSERC) and the Canada Foundation for Innovation (CFI).

out the polymerization using a differential monomer feeding technique.[5,6] Differential microemulsion polymerization includes three steps: (i) an initial period in which a mixture of initiator and surfactant in the recipe is heated in the reactor; (ii) an addition period over which the total monomer is added to the reactor; and (iii) an aging period to allow for complete polymerization of the unreacted monomer. He et al.[5] were the first group to report on the differential microemulsion polymerization technique. The reports on differential microemulsion polymerization indicate that this operation leads to an increase in the polymer/surfactant ratio, keeping particle size in the range of 15 nm, and homogeneous nucleation was proposed.[5,6] Nevertheless, to minimize particle size and surfactant in this type of homogeneous polymerization, it is necessary to operate under the so-called monomer-starved conditions during the addition period. However, high concentrated polymer nanoparticle emulsions with particle size of around 15 nm were not successfully achieved because of the extension of particle size by the aggregation of oligomers during propagation in the aqueous phase.[5] So the utilization of an oil-soluble initiator instead of the water soluble initiator will probably prevent the aggregation of oligomers during polymerization since heterogeneous nucleation possibly predominates throughout the reaction and a highly concentrated polymer nanoparticle emulsion can probably be obtained. Additionally, differential microemulsion polymerization via a two-step process was previously used to give polymer nanoparticles of poly(methyl methacrylate)/polystyrene (PMMA/PS).[7,8] Thus, the differential microemulsion polymerization is possibly an effective method to prepare the core/shell structure of glycidyl-functionalized PMMA latex nanoparticles having a high density of glycidyl functional groups on the surface. Azo-bis-isobutyronitrile (AIBN) an oil-soluble initiator is the selected initiator for synthesis of the core/shell nanostructure as has been reviewed in previous literature.[9-15] High molecular weight syndiotactic PMMA latex nanoparticles were obtained via polymerization of the MMA monomer using the modified microemulsion polymerization method with AIBN as an oil-soluble initiator.[14,15]

Thus, the preparation of core/shell structure of glycidyl-functionalized PMMA latex nanoparticles was studied in the present investigation by utilization of differential microemulsion polymerization via a two-step process using AIBN, as an oil-soluble initiator. This article reports on a statistical analysis of a full factorial experimental design for the synthesis of glycidyl-functionalized PMMA latex nanoparticles using differential microemulsion polymerization via a two-step process.[7,8] The effects of monomer/comonomer ratios, amounts of surfactant and water contents on the conversion of core/shell nanoparticles were studied. A factorial design of 2^3 experiments is used in the studies. The effects of the three process variables for the differential microemulsion polymerization, namely the MMA/GMA ratio, the amount of the surfactant and water content, on the conversion were investigated. Besides, the particle size and particle size distribution, molecular weight and polydispersity index of the copolymer were also measured.

EXPERIMENTAL

Materials

Commercial MMA was obtained from the Thai MMA, (Rayong, Thailand) and used without further purification. Commercial grade GMA supplied by Dow Chemical, (Middleborough, UK) was used as a comonomer without any purification. Azo-bis-isobutyronitrile (AIBN) was obtained from Siam Chemical Industry, and sodium dodecyl sulfate (SDS) from Cognis (Bangkok, Thailand), was used as received. High quality deionized water obtained from the FabriNet (Patumthanee, Thailand), was used in all experiments.

Factorial design experiment

A recipe for the differential microemulsion copolymerization of MMA/GMA copolymers is presented in Table I. A 2^3 factorial design is given in Table II and eight experiments with "+" for a high level and "−" for a low level expressed as variable identification are given in Table III. The variables understudy, GMA, SDS and water are given as variable 1, 2, and 3, respectively. The high levels of GMA, SDS and water variables are 4 cm^3, 1.4 g and 84 cm^3, respectively, while the low levels are 2 cm^3, 0.7 g and 60 cm^3, respectively.

Synthesis of core/shell copolymeric nanoparticles by differential microemulsion polymerization technique

Copolymeric nanoparticles were synthesized by differential microemulsion polymerization of MMA and GMA using AIBN as an initiator and SDS as a surfactant in a 250 cm^3 four-necked flat-bottomed flask equipped with a condenser, two dropping funnels, a nitrogen inlet capillary tube and a magnetic stirring bar immersed in a water bath. The stirrer speed was 200 rpm, the reaction temperature was 75°C, monomer feeding time was 2 h, and the subsequent reaction time was 1 hour. The sequence of monomer feeding was to prepare PMMA first and then prepare the copolymer of PGMA-*ran*-PMMA. The basic experimental procedures were as follows: The deionized water, initiator and SDS emulsifier

TABLE I
Recipe for a Differential Microemulsion Copolymerization of MMA/GMA Copolymers

Materials	Amount
MMA (cm^3)	14
GMA	Variable
AIBN (g)	0.08
SDS	Variable
Water	Variable

were charged into a 250-cm^3 glass reactor. The reactor was immersed in a water bath having a reaction temperature of 75°C. The reaction was stirred at 200 rpm by an elliptical shaped magnetic bar. After the reaction temperature had reached 75°C, MMA monomer (14 cm^3) was dropped into the reaction at a constant rate for 1½ h. Then GMA monomer (2 cm^3 or 4 cm^3) was dropped into the reaction mixture within 30 min. The reaction proceeded for another 1 h at 75°C under the constant reaction temperature and stirrer speed

The poly[(methyl methacrylate)-*ran*-(glycidyl methacrylate)] particles were obtained by precipitating the microemulsion polymers in methanol and filtering by a vacuum filtration technique, washing the precipitates with excess methanol and deionized water to remove the SDS emulsifier and AIBN oil-soluble initiator, and finally drying in a vacuum oven at 40°C for 24 h.

Characterization of the copolymers

The solid content and the monomer conversion

The solid content and conversion of the copolymer microemulsions were determined by the weight difference as shown in eqs. (1) and (2):

$$\% \text{ Solid} = (W_1/W_2) \times 100\% \quad (1)$$

$$\% \text{ Conversion} = (W_1/W_3) \times 100\% \quad (2)$$

where W_1, W_2, and W_3 were weights of the dried copolymer, latex formed, and the total monomers used, respectively. The dried copolymer was a pure copolymer after removing the initiator, surfactant, and residual monomer by washing with excess methanol and deionized water.

TABLE II
A 2^3 Factorial Design

	Variables		
Run	GMA (1)	SDS (2)	Water (3)
1	−	+	−
2	+	−	−
3	+	−	+
4	+	+	−
5	−	−	−
6	−	−	+
7	−	+	+
8	+	+	+

+ means a high level, − means a low level.

TABLE III
Variable Identification

Variables	− (Low level)	+ (High level)
GMA (cm^3)	2	4
SDS (g)	0.7	1.4
Water (cm^3)	60	84

MMA was fixed at 14 cm^3.

Particle size and particle size distribution

Particle size and particle size distribution were determined by means of a dynamic light scattering technique in a Zetasizer nano ZS Malvern Instrument (Worcestershire, UK) equipped with a He-Ne laser source at a wavelength of 633 nm and purified deionized water was used as a dispersing medium. The microemulsion copolymer was diluted to 1% w/v before analysis.

Molecular weights and their polydispersity index (PDI)

The weight and number average molecular weights as well as the polydispersity index (PDI) were determined by gel permeation chromatography (GPC Water 150-CV, Waters Associates, Milford, MA) equipped with a column set of PLgel, 10 μm mixed bed (two columns) having a molecular weight resolving range of 500–10,000,000 g mol^{-1} at a flow rate of 1 cm^3 min^{-1} at 30°C and tetrahydrofuran was used as an eluent. A calibration curve was constructed using standard polystyrene having a molecular weight range of 4490 to 1,112,000 g mol^{-1}. The dried copolymer was dissolved in tetrahydrofuran at a concentration of 0.3% w/v and then filtered with a nylon membrane (pore size 0.45 μm) before injection.

Morphology of the core/shell nanoparticles

Morphology of the core/shell copolymeric nanoparticles was investigated by transmission electron microscopy. The copolymer emulsion was diluted to 1%, v/v; then one drop of this diluted emulsion was placed on a copper grid, negatively stained by phosphor tungstic acid and dried at room temperature. Another dried copolymer was stained with OsO_4 vapor at room temperature for 60 min and was then carefully dispersed in an epoxy matrix, cured at room temperature, and microtomed to obtain ultrathin specimens. Both the negatively stained

TABLE IV
Summarized Data of PMMA Core Nanoparticles

	2^3 full factorial experiment											
				Design level			Response	Observe				
Run	[GMA] (cm^3)	[SDS] (g)	[Water] (cm^3)	[GMA]	[SDS]	[Water]	% Conversion	$\overline{M}_n \times 10^{-6}$	$\overline{M}_w \times 10^{-6}$	PDI	Size (nm)	PSD
1	−	1.4	60	none	+	−	83.77	0.24	0.63	2.70	24.76	0.249
2	−	0.7	60	none	−	−	79.61	0.28	0.78	2.80	41.40	0.448
3	−	0.7	84	none	−	+	83.55	0.23	0.69	2.90	32.16	0.267
4	−	1.4	60	none	+	−	83.77	0.24	0.63	2.70	24.76	0.249
5	−	0.7	60	none	−	−	79.61	0.28	0.78	2.80	41.40	0.448
6	−	0.7	84	none	−	+	83.55	0.23	0.69	2.90	32.16	0.267
7	−	1.4	84	none	+	+	89.16	0.23	0.57	2.50	30.07	0.379
8	−	1.4	84	none	+	+	89.16	0.23	0.57	2.50	30.07	0.379

PDI, polydispersity index of molecular weights and PSD, particle size distribution; MMA, 14 cm^3.

samples on the copper grid and ultra-thin cross-sectioned specimens were observed using a transmission electron microscope (TEM, Joel JEM-200CX, Tokyo, Japan).

RESULTS AND DISCUSSION

The statistical analysis in this work was performed using Program Minitab version 13.20. All of the statistical values were also calculated by the program. In addition, the confidence level of all experiments was set at 95%. The heterogeneous nucleation mechanism was believed to predominantly control both the PMMA core polymerization and the core/shell copolymerization. The summary of all data is shown in Tables IV and V.

The summarized data in Tables IV and V indicate that $\overline{M}_w$ and $\overline{M}_n$ of the PMMA core nanoparticles in every run were not very different. Since MMA monomers were polymerized inside the micelles within the SDS solution, chain transfer from the PMMA growing chains or disproportionation transfer to the MMA monomer was a major termination step rather than a normal combination of the two PMMA growing chains to become a larger PMMA chain. Thus, the similar chain growth and chain termination provided the similar $\overline{M}_w$, $\overline{M}_n$ and PDI of the PMMA core nanoparticles. In addition, the conversion of the core/shell nanoparticles increased as expected when the shell layer was formed by the copolymerization. Thus, $\overline{M}_w$ of the core/shell nanoparticles increased along with the conversion. The $\overline{M}_n$ of the core/shell nanoparticles decreased because the GMA oligomers in the aqueous phase probably homopolymerized and precipitated but the micelles remained intact before further chain growth and/or chain termination could take place. Therefore, the PDI of the core/shell nanoparticles was increased.

A marked difference between the particle size as shown in Tables IV and V indicates that with an increase in the amount of surfactant, the particle size and size distribution decreased for the MMA polymerization For the MMA polymerization, particle size significantly depends on the nucleation conditions. A high surfactant concentration would result in a higher particle population with a smaller particle size. However, the copolymer particle size and

TABLE V
Summarized Data of Core/Shell Nanoparticles

	2^3 full factorial experiment											
				Design level			Response	Observe				
Run	[GMA] (cm^3)	[SDS] (g)	[Water] (cm^3)	[GMA]	[SDS]	[Water]	% Conversion	$\overline{M}_n \times 10^{-6}$	$\overline{M}_w \times 10^{-6}$	PDI	Size (nm)	PSD
1	2	1.4	60	−	+	−	92.59	0.20	1.50	7.60	25.69	0.264
2	4	0.7	60	+	−	−	89.53	0.15	0.49	3.30	29.83	0.276
3	4	0.7	84	+	−	+	90.67	0.19	0.56	2.90	27.67	0.250
4	4	1.4	60	+	+	−	88.51	0.20	0.60	3.10	38.33	0.439
5	2	0.7	60	−	−	−	92.24	0.21	2.20	10.40	25.40	0.280
6	2	0.7	84	−	−	+	98.42	0.18	0.61	3.40	29.49	0.268
7	2	1.4	84	−	+	+	99.55	0.17	0.78	4.50	38.65	0.415
8	4	1.4	84	+	+	+	92.02	0.19	0.79	4.20	24.79	0.270

PDI, polydispersity index of molecular weights and PSD, particle size distribution; MMA, 14 cm^3.

TABLE VI
Factorial Fitted Results of the Conversion of PMMA Core Nanoparticles

Term	Effect	Coef	SE coef	*T*	*P*	
Constant		84.0250	0.03021	2781.58	0.000	
[GMA]	0.0000	0.0000	0.03021	0.00	1.000	
[SDS]	4.8833	2.4417	0.03021	80.83	0.000	
[Water]	4.6633	2.3317	0.03021	77.19	0.000	
[GMA]*[SDS]	0.0000	0.0000	0.03021	0.00	1.000	
[GMA]*[Water]	0.0000	0.0000	0.03021	0.00	1.000	
[SDS]*[Water]	0.7233	0.3617	0.03021	11.97	0.000	
[GMA]*[SDS]*[Water]	0.0000	0.0000	0.03021	0.00	1.000	
Source	DF	Seq SS	Adj SS	Adj MS	F	P
Main Effects	3	273.562	274.562	91.1872	4163.80	0.000
Two-way interactions	3	3.139	3.139	1.0464	47.78	0.000
Three-way interactions	1	0.000	0	0.0000	*	*
Residual error	16	0.350	0.35	0.0219		
Pure error	16	0.350	0.35	0.0219		
Total	23	277.051				

S = 0.147986; R-Sq = 99.87%; R-Sq (adj) = 99.82%.

size distribution increased significantly with increasing [SDS] concentration as seen in Runs 4 and 7 (Table V) which is in contrast with the rest of the experiments. Based on this observation, it is possible that aggregation of the copolymer could take place which may be caused by an insufficient amount of [SDS] at higher amounts of GMA and water.The particle size and particle size distribution of the core/shell nanoparticles were almost in the same range with the PMMA core particles since the copolymerization was possibly dominated by the reaction between the fed GMA and swollen MMA in the polymer micelles and then a small amount of the comonomer was not affected by the particle size and size distribution.

Statistical analysis

PMMA core nanoparticles

In Table VI, the statistical analyzed data of the conversion of the resultant PMMA core nanoparticles indicated that the conversation was significantly affected by [SDS], [water], and their interaction.

The SDS micelles were the important nucleation sites for the heterogeneous nucleation mechanism, since the high SDS content provided a high amount of micelles. Thus the conversion depended on the amount of SDS micelles. The effect of the water content was related to the aggregation of polymer nanoparticles during polymerization when small amounts of water were used since this condition provided a high chance for micelle aggregation. It can be concluded that the conversion was also dependent upon the water content. In addition, the interaction between the amounts of SDS and water could be attributed to the stability of the polymer micelles. Therefore, the interaction between SDS and water is also an important factor influencing the conversion. Figure 1 indicates the positive effects of the contents of SDS and water, and their interaction on the conversion of the resultant PMMA core nanoparticles.

The SDS, an anionic surfactant, usually stabilizes the monomer droplets through a micelle formation and subsequently leads to stable polymer micelles. As differential microemulsion polymerization proceeds, the polymer micelles were always swollen with its monomer. Increasing the number of monomer-swollen polymer micelles, as the polymerization proceeds, can increase the monomer conversion, i.e., the higher the SDS concentration, the greater the monomer conversion. When increasing the amount of water charged to the system, a higher conversion of monomer was observed because chain transfer from the PMMA growing chains to the MMA monomer was a major termination step rather than a normal combination of the two PMMA growing chains

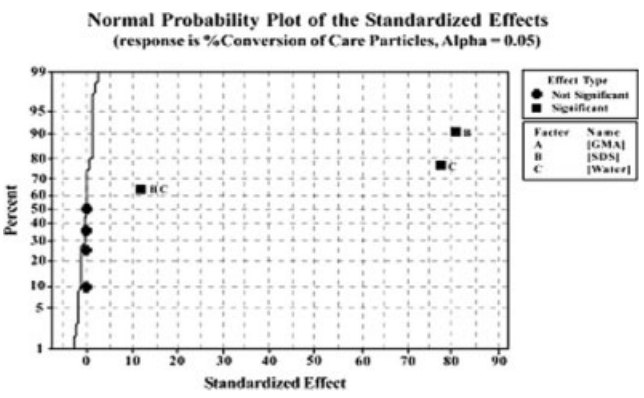

Figure 1 Normal probability plot of the standardized effects for PMMA core nanoparticles.

TABLE VII
Factorial Fitted Results of the Conversion of Core/Shell Nanoparticles

Term	Effect	Coef	SE Coef	*T*	*P*	
Constant		92.941	0.03449	2694.69	0.000	
[GMA]	−5.517	−2.758	0.03449	−79.97	0.000	
[SDS]	0.453	0.227	0.03449	6.57	0.000	
[Water]	4.447	2.223	0.03449	64.46	0.000	
[GMA]*[SDS]	−0.292	−0.146	0.03449	−4.23	0.001	
[GMA]*[water]	−2.118	−1.059	0.03449	−30.71	0.000	
[SDS]*[water]	0.785	0.393	0.03449	11.38	0.000	
[GMA]*[SDS]*[water]	0.400	0.200	0.03449	5.80	0.000	
Source	DF	Seq SS	Adj SS	Adj MS	*F*	*P*
Main effects	3	302.472	302.472	100.8240	3531.49	0.000
Two-way interactions	3	31.132	31.132	10.3770	363.48	0.000
Three-way interactions	1	0.960	0.96	0.9600	33.63	0.000
Residual error	16	0.457	0.457	0.0290		
Pure error	16	0.457	0.457	0.0290		
Total	23	335.020				

S = 0.168967 R−Sq = 99.86% R-Sq (adj) = 99.80%.

to become a larger PMMA chain. Thus, a higher amount of MMA monomer was consumed. The second role of water is to dilute the ingredients of the polymerization system and reduce the polymerization reaction and a smaller chance of polymer micelle aggregation. As mentioned in the factorial design experiment, the interaction effect of SDS and water content increased the monomer conversion; a synergistic effect between the SDS and water could additionally be attributed to the stability of the polymer micelles in the presence of SDS, which reduced the micelle aggregation, and perhaps reduced or inhibited chain termination by combination.

Core/shell nanoparticles

In Table VII, the statistical analysis of the percentages of the resultant core/shell nanoparticles indicate that the conversion is significantly affected by the contents of SDS, water, GMA, and their interactions (the two- and three-way interactions). Based on the values of *T* and *p* statistic analysis and Figure 2, all variables studied affected the conversion of core/shell nanoparticles since the random copolymer between MMA and GMA was possibly copolymerized at the surface of PMMA core nanoparticles inside the SDS micelles. In addition, the water content had an influence on the aggregation of the polymer micelles. The parameters of SDS and water, and their two-way interaction gave a positive effect on conversion, while GMA and its two-way interaction with SDS and water gave a negative interaction. This is very interesting in that the three-way interaction among the GMA, SDS, and water provided a weakly positive result. It is anticipated that the effect of SDS and water overwhelms the strong negative effect of GMA.

GMA is a better water soluble monomer (its solubility in water = 50 g dm^{-3} at 25°C) than MMA (its solubility in water = 15 g dm^{-3} at 25°C) and thus GMA can polymerize more in the aqueous phase via free radicals generated from the chain termination by chain transfer to monomer or from the free radical of AIBN left in the system. However, the homopolymerization of GMA in the emulsion system was not as good as discussed elsewhere because of the amount of AIBN free radicals in the aqueous phase.[16] In addition, the PMMA core nanoparticles were nucleated inside the surfactant micelles and thus the precipitation of GMA oligomers on PMMA core nanoparticles could be affected by the SDS micelle around the particles. Therefore, GMA could possibly be copolymerized with MMA droplets swollen in the polymer micelles and/or an active chain end of the polymer micelles to form a shell layer of a random copolymer between MMA and GMA.[13,17] Moreover, the effect of water content

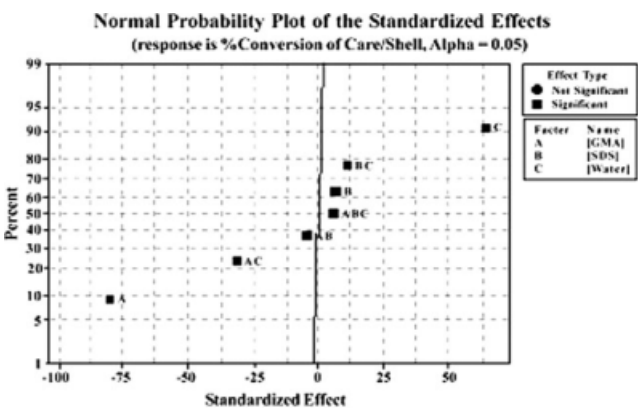

Figure 2 Normal probability plot of standardized effects and residual plot for conversion of core/shell particle copolymerization.

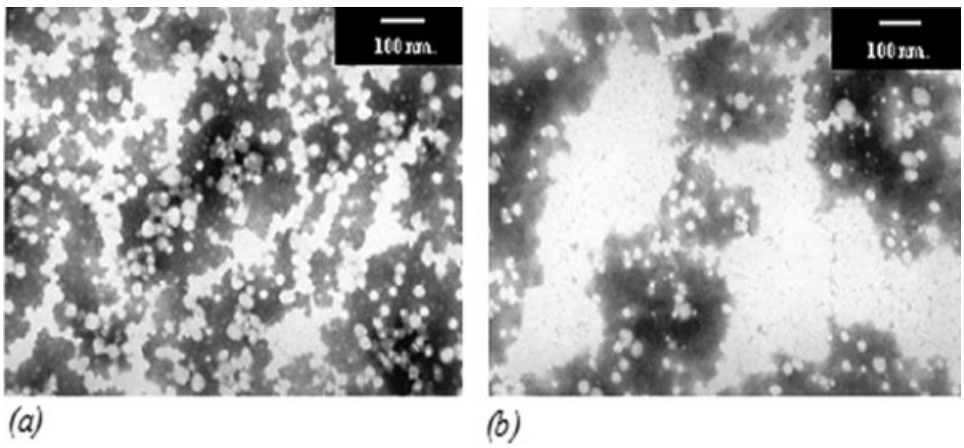

Figure 3 Transmission electron micrographs: (a) PMMA core particle, and (b) core/shell nanoparticles.

probably came from the extent of aqueous phase polymerization of GMA as mentioned earlier. For the polymerizations carried out in the differential microemulsion polymerization, the GMA content, interaction between GMA and water, and GMA and SDS gave a negative effect on conversion. The former was caused by the waste amount of GMA in the aqueous phase while the latter by the shielding of SDS which prevented its copolymerization with PMMA core particles. The extent of the negative effect on the interaction between GMA and water was larger than that between GMA and SDS.

Morphology study

The white particles and aggregated particles are obvious from the negative staining as shown in Figure 3. The PMMA core nanoparticles in Figure 3(a) and the copolymer nanoparticles in Figure 3(b) have a spherical shape. In addition, the high concentration of the polymer sample caused the aggregation of polymer nanoparticles as presented in both micrographs which is due to the small amount of SDS or interaction between the hydrophilic homopolymer of GMA and water. The reactivity ratios of GMA and MMA are 1.28 and 0.75, respectively[18], therefore, the product of r_{MMA} and r_{GMA} equals 0.96, an indication of a random copolymer. Therefore, the copolymer latex nanoparticle is believed to be composed of a nano-seed of PMMA nanoparticle and the poly-[(methyl methacrylate)-*co*-(glycidyl methacrylate)][3,19,20] as a shell layer on the surface of the PMMA nano-seed. Our present result having the very thin layer of PGMA agrees well with that observed by Chen and Lee[3]. They found that the higher reactivity of GMA over that of MMA caused GMA to copolymerize with MMA inside the PMMA core leaving less density of PGMA on the copolymer surface.

However, the TEM in Figure 4 illustrates, more or less, the very diffuse nanostructure of the PMMA core particle and the random copolymer of poly-(GMA-*ran*-MMA) at the shell layer as observed by a very thin gray line surrounding the nanoparticle since the glycidyl functional group on the surface of the core/shell nanoparticles could react with osmium tetroxide staining agent to the same degree as for the PMMA core nanoparticles.

CONCLUSIONS

Functionalized core/shell nanoparticles of MMA/GMA copolymer could be polymerized via the technique of differential microemulsion polymerization. The synthesis of the core/shell nanoparticles involves low surfactant usage at a weight ratio of SDS/monomer of 1 : 24, can reach a high conversion (80–90%) to form the product with high molecular weight of $\overline{M}_n$ from 2.4 to 3 $\times$ 10^5 g mol^{-1} and $\overline{M}_w$ from 6–8 $\times$ 10^5 g mol^{-1}, and a small particle size of around 25–30 nm. The statistical analysis indicated that [SDS], [water], and their two parameter interaction have significant positive effects on the conversion of PMMA core nanoparticles. The [GMA],

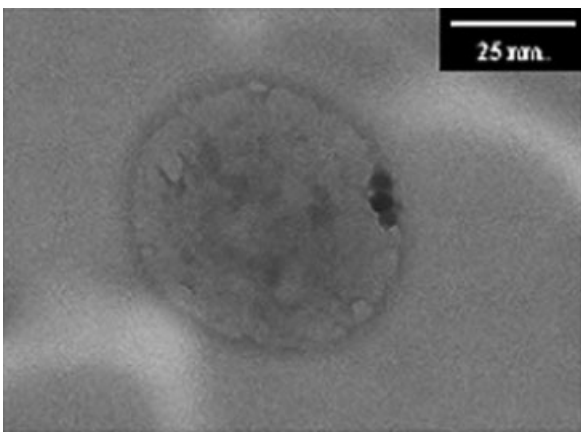

Figure 4 Transmission electron micrograph of cross-sectioned surface of the dried core/shell particle in run 6.

[GMA]*[SDS], and [GMA]*[water] gave significant negative effects on conversion, On the other hand, the single parameter effect of [SDS] and [water], the two parameter interaction of [SDS] and [water], and the three parameter effect of [GMA]*[SDS]*[water] have significant positive effects on the conversion of core/shell nanoparticles.

References

1. Kawaguchi, H. Prog Polym Sci 2000, 25, 1171.
2. Pichot, C. Curr Opion Colloid Interface Sci 2004, 9, 213.
3. Chen, C.-H.; Lee, W.-C. J Polym Chem Part A: Polym Chem 1999, 37, 1457.
4. Pavel, F. M. J Dispersion Sci Technol 2004, 25, 1.
5. He, G.; Pan, Q.; Rempel, G. L. Macromol Rapid Commun 2003, 24, 585.
6. He, G.; Pan, Q.; Rempel, G. L. Ind Eng Chem Res 2007, 46, 1682.
7. He, G.; Pan, Q.; Rempel, G. L. J Appl Polym Sci 2007, 105, 2129.
8. He, G.; Pan, Q. Macromol Rapid Commun 2004, 25, 1545.
9. Roy, S.; Devi, S. J Appl Polym Sci 1996, 62, 1509.
10. Gan, L. M.; Chews, C. H.; Ng, S. C.; Loh, S. E. Langmuir 1993, 9, 2799.
11. Rodriguez-Guadarrama, L. A.; Mendizabal, E.; Puig, J. E.; Kaler, E. W. J Appl Polym Sci 1993, 48, 775.
12. Gan, L. M.; Lee, K. C.; Chew, C. H.; Tok, E. S.; Ng, S. C. J Polym Sci Part A: Polym Chem 1995, 33, 1161.
13. Ming, W. H.; Jones, F. N.; Fu, S. K. Polym Bull 1998, 40, 749.
14. Ming, W. H.; Jones, F. N.; Fu, S. K. Macromol Chem Phys 1998, 199, 1075.
15. Pilcher, S. C.; Ford, W. T. Macromolecules 1998, 31, 3454.
16. Pichot, C. Macromol Symp 1990, 35, 327.
17. Pichot, C. Polym Adv Technol 1995, 6, 427.
18. Brandrup, J.; Immergut, E. H. Polymer Handbook, 4th ed.; Wiley: New York, 1999.
19. Ergozhin, E. E.; Bektenov, N. A.; Chopabaeva, N. N. Russ J Appl Chem 2004, 77, 813.
20. Hild, G.; Lamps, J. P.; Rempp, P. Polymer 1993, 34, 2875.